

## CHARACTERIZATION OF SINGLE WALL CARBON NANOTUBES SYNTHESIZED BY KrF EXCIMER LASER ABLATION IN NITROGEN ATMOSPHERE

J. AL-ZANGANAWEE<sup>a,b\*</sup>, C. MOISE<sup>a</sup>, A. KATONA<sup>a</sup>, D. BOJIN<sup>a</sup>,  
M. ENACHESCU<sup>a</sup>

<sup>a</sup>*Center for Surface Science and Nanotechnology (CSSNT), University Politehnica of Bucharest, Romania*

<sup>b</sup>*Physics Department, College of Science, University of Diyala, Iraq*

We report the fabrication of single wall carbon nanotubes (SWCNTs) by KrF excimer laser ablation under nitrogen atmosphere with a yield of over 70%. We used for the ablation process KrF excimer laser with a 20 ns pulse period and 30 Hz repetition rate, oven temperature 1100 °C, target composition: 0.6 at% Ni, 0.6 at% Co, 98.8 at% C (atomic percentage), 300 L/h nitrogen gas flow rate and a pressure of 500 Torr. Raman spectroscopy, transmission electron microscopy (TEM), scanning electron microscopy (SEM), and thermogravimetric analysis (TGA) measurement results showed that the produced nanotubes have high length, narrow diameter distribution and contain low amount of amorphous carbon and metal catalyst particles.

(Received August 10, 2015; Accepted October 5, 2015)

*Keywords:* Single wall carbon nanotube, Excimer laser ablation, Nitrogen gas, Raman micro-Spectroscopy, TEM, SEM, TGA

### 1. Introduction

Since their discovery in the early 1990s carbon based nanomaterials, especially single wall carbon nanotubes (SWCNTs) are still captivating the interests of plenty scientific groups and industries all over the world, due to their physical and chemical properties. Among the most important applications of SWCNTs we highlight the fabrication of biosensors [1,2,3], scanning microscope tips [4], third generation solar cells [5] and nano-electronics [6], as well as they being good candidate for hydrogen storage.

Many different techniques have been used for the fabrication of single wall carbon nanotubes (SWCNTs). Chemical vapour deposition (CVD) [7], arc discharge [8], and laser ablation techniques [9] have been used as the main methods for producing SWCNTs. Pulse laser ablation (PLA) method was observed to produce high quality and high purity single wall carbon nanotubes. Many different parameters such as ablation temperature, laser wavelength, laser energy, pressure, type of the inert gas, etc., have been studied for optimizing laser ablation method for producing SWCNTs [10]. Different techniques such as Raman spectroscopy [14], Transmission Electron Microscopy (TEM) [15], and Scanning Electron microscopy (SEM) [15], Thermogravimetric analysis (TGA) [16] have been used for the characterization of the ablation product. Many researchers have been used excimer laser ablation technique for synthesizing SWCNTs in argon atmosphere [11, 12, 13].

The novelty of this work consist of using excimer laser instead of other lasers in nitrogen atmosphere as a carrier gas for producing of high quality single wall carbon nanotubes with long length and narrow diameter distribution.

---

\* Corresponding author: jasim\_mansoor@yahoo.com

## 2. Experimental work

The laser ablation experiments were carried out in a custom-designed installation depicted in Fig.1. [10,13]. This laser ablation apparatus was developed by Professor Enachescu's group. The experimental conditions for the production of SWCNTs are shown in the Table.1.

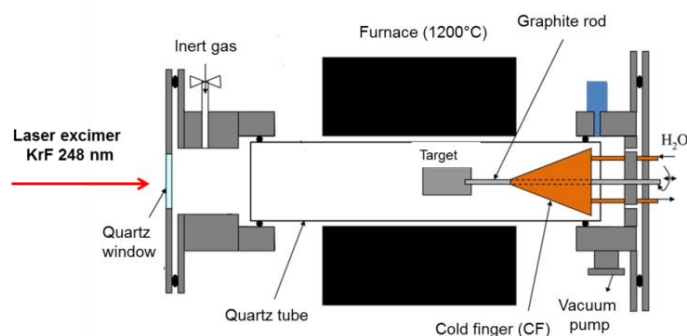


Fig 1. Ablation chamber apparatus design.

The laser ablation starts by passing the laser beam through a UV transparent quartz window and enters into the quartz tube hitting the target, when the target material begins to be ablated. The target was rotated during ablation with constant speed to get uniform ablation. Then the inert gas, which enters from the left-up side of the reaction chamber, moves through the quartz tube to the heated area where the reaction takes place, transporting the ablation product toward a copper condenser called cold finger (CF), where it will be deposited as a black soot. The cold finger was cooled down using water at 12 °C supplied by a chiller. The quartz tube of the reaction chamber was 1260 mm long, with the inner diameter of 50 mm. The inert atmosphere and the transportation of the ablated material within the tube to the CF were maintained by using nitrogen gas with 300 L/h flow rate. The experimental parameters were optimized in our lab in some earlier studies [10, 13, 17].

Table 1: Laser ablation parameters

No	Parameter	Value
1	Laser type	Excimer KrF, 248 nm
2	Laser energy	610 mJ
3	Repetition rate	30 Hz
4	Pulse length	20 ns
5	Area of Laser beam spot	20 mm <sup>2</sup>
6	Oven temperature	1100 °C
7	Gas Pressure	500 Torr
8	Ablation time	60 minute

The targets were prepared following an original recipe developed in our laboratory, by mixing a graphite cement (GC 8010-B from Metal Forming Lubricants) with metal micro sized powder of Ni and Co (Sigma Aldrich), in the following atomic ratio C/Ni/Co = 98.8/0.6/0.6. The resulting mixture was transferred into a Teflon mould (20 mm diameter), then cured at 130°C for 4 hours in air to improve the mechanical strength. Then it was followed by a heat treatment at 800°C in an inert atmosphere for one hour to remove all the remaining organic compounds. Finally it was obtained a target containing only carbon, nickel and cobalt atoms in the ratio mentioned above.

The collected product was investigated using confocal micro-Raman spectroscopy, thermogravimetric analysis (TGA), transmission electron microscopy (TEM), and scanning electron microscopy (SEM).

### 3. Results and Discussions

#### 3.1 Characterization by confocal micro-Raman spectroscopy

The products obtained have also been characterized by the confocal Raman micro-spectroscopy with a Horiba Labram 800, using 532 nm and 633 nm laser excitation wavelengths. The spectra of the ablation products (Fig.2A) were compared with those of the commercial SWCNT from Sigma (Fig.2B). In the Raman spectra we distinguish three main regions specific to SWCNTs: radial breathing mode (RBM), D band and G bands which were further analysed.

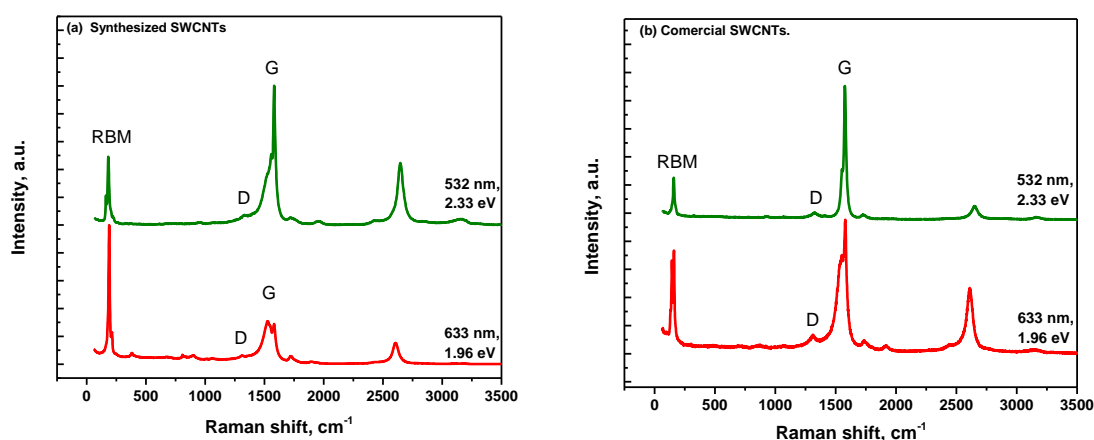


Fig 2: (a) Raman spectra of the raw ablation product recorded with red (633nm) and green laser (532 nm). (b) Raman spectra of the commercial SWCNTs recorded with red (633nm) and green laser (532 nm).

##### 3.1.1 RBM band analysis

The radial breathing mode (RBM) of SWCNTs from the ablation product and commercial SWCNTs are shown in Figure 3. For our product using the green laser, we found two peaks corresponding to two diameters distribution, while using the red laser only one peak was found as shown in the Table 2. For the commercial product using the green laser, one peak was found corresponding to a single diameter distribution, while using the red laser two peaks were found as shown in the Table 2. The vibrational frequency in the radial direction strongly depends with the diameter of the nanotube, described by the equation 1 [11]:

$$d = c1/(\omega - c2) \quad (1)$$

Where  $\omega$  - frequency for vibrations in the radial direction [ $\text{cm}^{-1}$ ],  $c1$ ,  $c2$  – are constants [ $\text{cm}^{-1}$ ];  $c1 = 215$  [ $\text{cm}^{-1}$ ] and  $c2 = 18$  [ $\text{cm}^{-1}$ ], and  $d$  is the diameter of the nanotube [nm]. The equation 1 was used to calculate the diameters of the SWCNTs and their values are summarized in the Table 2.

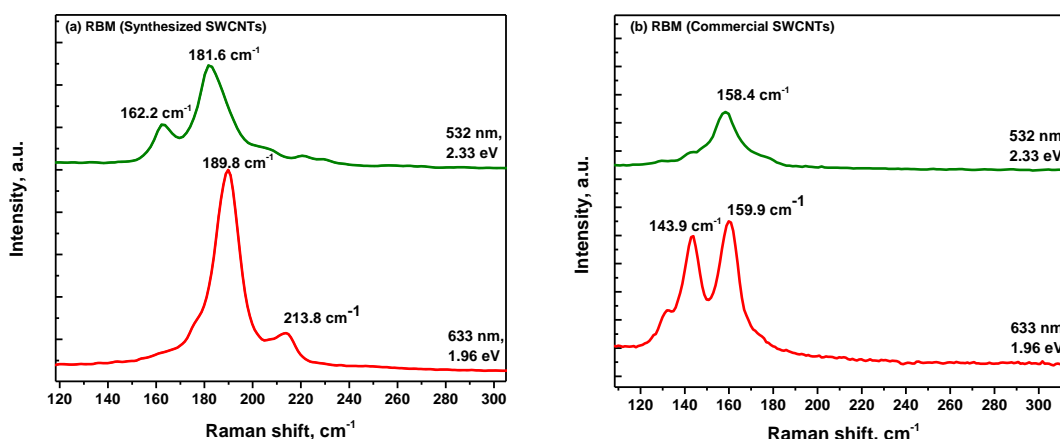


Fig 3. RBM band of the Raman spectra for the raw ablation product (a). RBM band of the Raman spectra for the commercial SWCNTs (b)

Table 2: Calculated diameters of the synthesized SWCNTs and commercial SWCNTs using Eq. 1

Type of Laser	Synthesized SWCNTs		Commercial SWCNTs	
	Vibration frequency [cm <sup>-1</sup> ]	SWCNTs diameter [nm]	Vibration frequency [cm <sup>-1</sup> ]	SWCNTs diameter [nm]
Green 532 nm (2.33eV)	162.2	1.49	158.4	1.53
	181.6	1.31		
Red 633 nm (1.96 eV)	189.8	1.25	143.9	1.71
	213.8	1.10		

The diameters of the individual nanotubes in the ablation product have been estimated to be between 1.10 nm and 1.49 nm. Similar values have been reported by other authors for the SWCNTs obtained by laser ablation of targets with a similar composition [12].

### 3.1.2 D and G band analysis

The D band from the Raman spectra is characteristic for the scattering on sp<sup>3</sup> carbon atoms, therefore this signal is assigned to the presence of the amorphous carbon in the sample and the defects in the structure of the carbon nanotubes, on the other hand the presence of G band is due to the scattering on sp<sup>2</sup> carbon from the structure of SWCNTs. Hence, the ratio of the integrated intensity of D and G bands,  $I_G/I_D$  is a measure of the SWCNTs quality: purity (amorphous carbon content) and defects of SWCNTs. The  $I_G/I_D$  area ratio of our produced SWCNTs was over 100 indicating high quality SWCNTs. The Raman spectra of both products indicated the presence of high quality SWCNTs (Fig.4A and Fig.4B), the laser wavelength having no influence on this ratio.

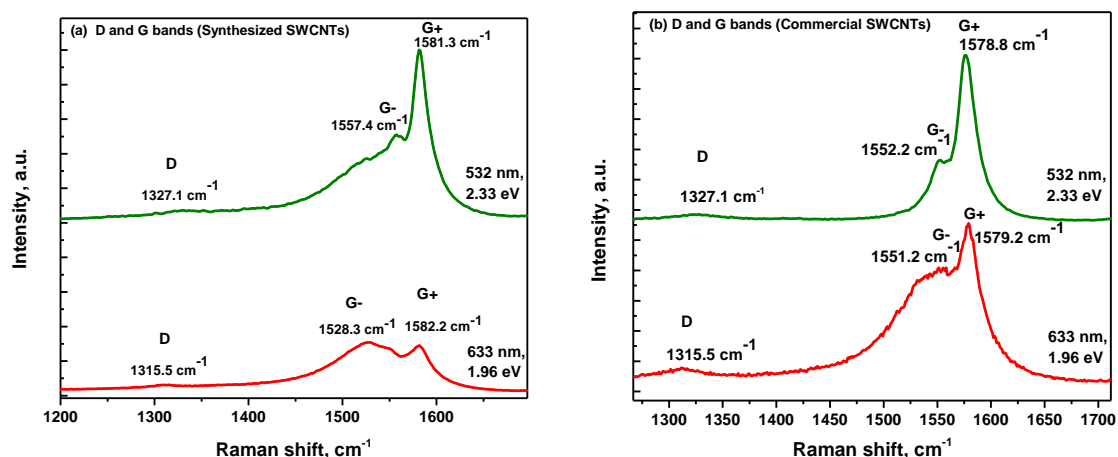


Fig 4. D and G bands of the Raman spectra recorded with red (633nm) and green laser (532 nm). (a) Raw ablation product. (b) Commercial SWCNTs

### 3.1.3 Kataura Plot analysis

The relationship between the diameter of single wall carbon nanotube and its band gap energy can be given by Kataura plot [13]. By using equation (1) and Kataura plot, the single wall carbon nanotubes can be characterized as metallic or semiconducting type depending on their diameter.

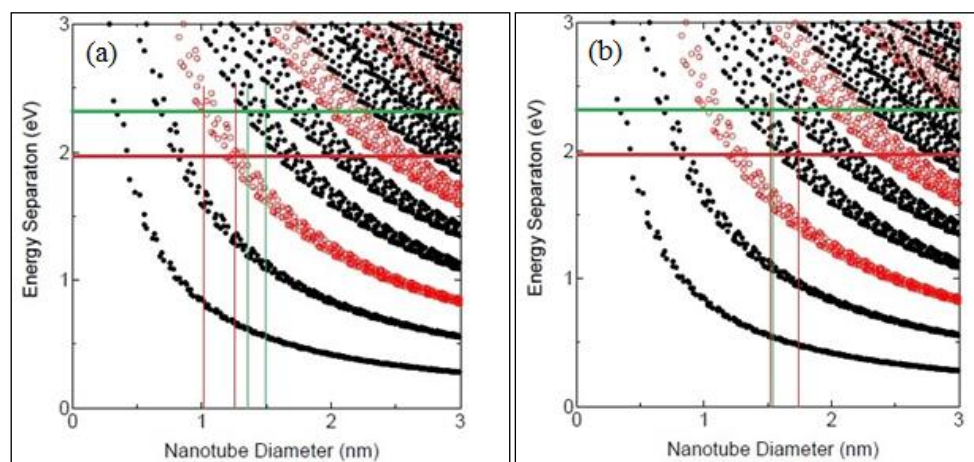


Fig 5. Kataura Plot with black points indicating semiconductor nanotubes and red circles indicating metallic nanotubes. The horizontal green line indicates the energy of the green laser (2.33 eV), while the red line the energy of the red laser (1.96 eV). (a) The vertical green lines indicate the diameter distribution of the nanotubes of our ablation product obtained with the green laser and the red line with the red laser [13]. (b) The vertical green lines indicate the diameter distribution of the commercial nanotubes from Sigma obtained with the green laser and the red line with the red laser [13].

## 3.2 Characterization by transmission electron microscopy and scanning electron microscopy

The typical transmission electron microscopy images of the unpurified raw ablation product can be shown in figure 7. The raw ablation product was dispersed in dimethylformamide (DMF) supplied from Sigma-Aldrich in an ultrasonic water bath for 8 hours to get good dispersion. Philips-EM 410 TEM was used to obtain micrographs of raw product dispersion. The micrographs showed that the SWCNTs found in the raw ablation product were grouped in bundles of different

diameters, with low content of metal catalysts and amorphous carbon. The TEM micrographs supported the Raman analysis data.

The typical TEM and SEM images of our raw ablation product are shown in figure 7 and 8. The SEM and TEM micrographs revealed the presence of micrometers long SWCNTs grouped in bundles of 10.2 nm-29.29 nm in diameter. Also these images show the presence of graphite, amorphous carbon and metal catalysts along with the SWCNTs.

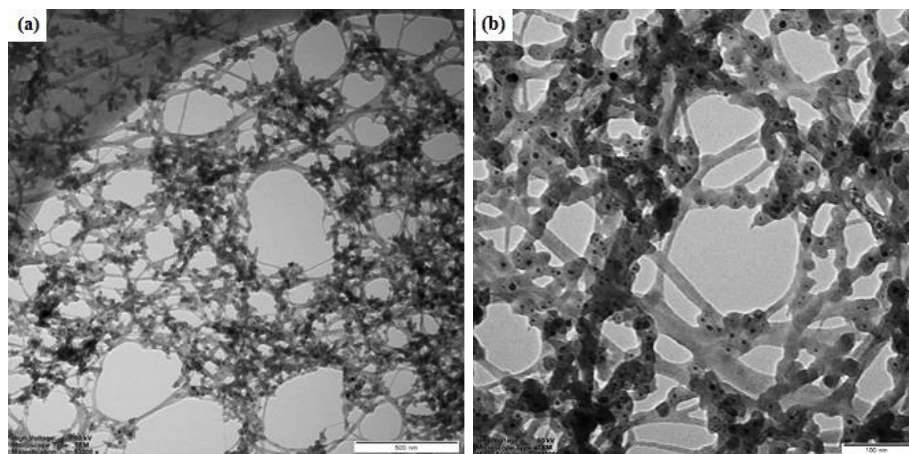


*Fig 7. Transmission Electron Microscopy (TEM) Micrographs of the raw ablation product. (a) TEM micrograph of raw product with high voltage 80 kV, magnification 53000 x and scale 500 nm. (b) TEM micrograph of raw product with high voltage 80 kV, magnification 190000 x and scale 100 nm.*

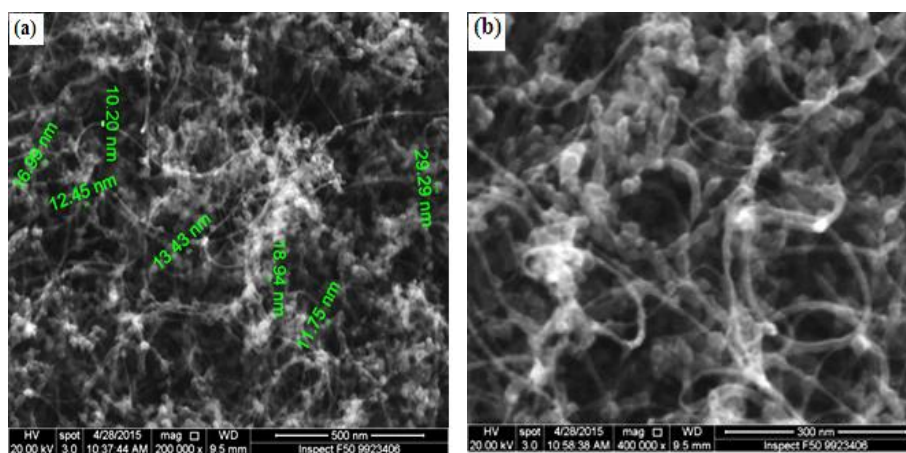


*Fig 8. Scanning electron microscopy (SEM) Micrographs of the raw ablation product. (a) SEM micrograph with 2000kV HV, 200000x magnification and 500 nm scale (b) SEM micrograph with 2000kV HV, 400000x magnification and 300 nm scale.*

### 3.3 Thermogravimetric analysis (TGA)

The thermogravimetric analysis (TGA) of the ablation product was carried out in air with a 5°C/min temperature ramp. The TGA curves for the ablation product, target and graphite cement were recorded (Fig.9 ). The TGA curve of the ablation product shows a burning slope centered around 377°C, while the target and graphite cement a slope centered around 700°C proving that a new product was formed during laser ablation. Higher residual mass resulted for the ablation product than for the ablated side of the target. Also the residual mass of the ablated side of the target is higher than that of the not ablated side of the target, showing that during ablation an increase of metal content at the target surface occurred.

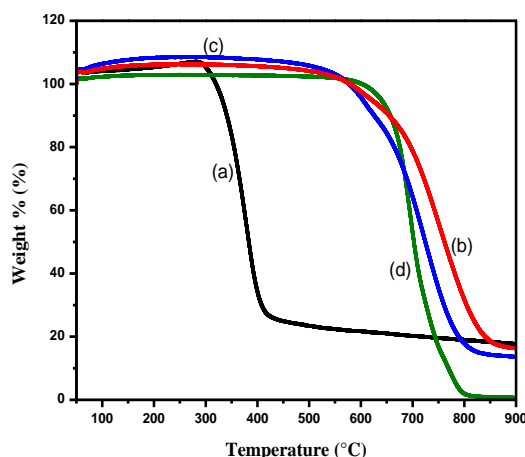


Fig 9. TGA curve recorded in air of the ablation product (a), ablated side of the target (b), not ablated side target (c), respectively the graphite cement (d). TGA conditions: air (20 mL/min), temperature: 100-900 °C, ramp: 5 °C/min

The TGA and its derivative curves (DTG) of our ablation product are shown in the Fig 10A a) and b). The DTG curve shows the presence of one peak with a maximum of oxidation rate at 377°C, when 80% of the product mass was lost, corresponding to SWCNTs and amorphous carbon. The peak indicates a very low content of amorphous carbon. Also no further peaks were observed in the derivative curve showing that no other byproduct was formed. The residual mass corresponding to the metal catalyst was 17.7%. From the TGA curve we estimate a yield of over 70% of the SWCNTs production.

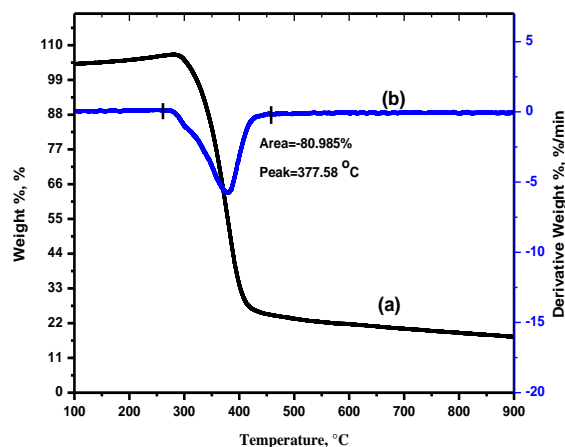


Fig 10A. TGA curve (a) and its derivative (b) of the raw ablation product TGA conditions: air (20 mL/min), temperature: 100-900 °C, ramp: 5 °C/min.

TGA and its derivative curves of the commercial SWCNTs are shown in the Fig 10B a) and b). The derivative of the TGA curve shows the presence of one peak with a maximum of oxidation rate at 439°C, when 56% of the product mass was lost, corresponding to SWCNTs. The peak indicates no content of amorphous carbon. Also no further peaks were observed in the derivative curve showing that no other by product was formed. The residual mass corresponding to metal catalyst was 44.5%. From the TGA curve we estimate a yield of over 50% of the SWCNTs production.

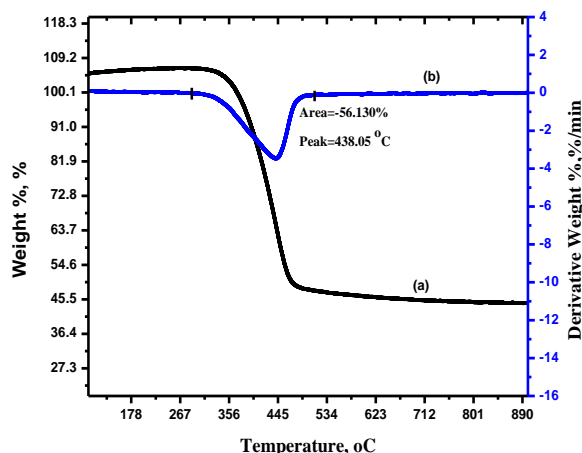


Fig 10B. TGA curve (a) and its derivative (b) of the commercial SWCNTs TGA conditions: air (20 mL/min), temperature: 100-900 °C, ramp: 5 °C/min.

We found that our SWCNTs have 27% lower metal catalyst content than commercial SWCNTs. Also we found that our product presents higher SWCNTs content with over 15% than the commercial one.

#### 4. Conclusions

In this work we have shown that the KrF excimer laser ablation in nitrogen atmosphere is a suitable method for the production of high quality single wall carbon nanotubes. The SWCNTs obtained in our work have narrow diameter distributions between 1.1 nm and 1.49 nm. Two types of SWCNTs were obtained metallic and semiconducting SWCNTs with high yield of over 70%. The method presented in this work is suitable for the production of metallic and semiconducting SWCNTs. The quality of the produced SWCNTs by this method was confirmed by Raman, TGA and TEM analysis showing low content of amorphous carbon and defects in the structure of the nanotubes. We have shown that our method was able to produce SWCNTs with higher yield and lower metal catalyst content than the commercial SWCNTs.

#### Acknowledgments

This work was supported by Romanian Ministry of Education and by Executive Agency for Higher Education, Research, Development and Innovation Funding, under projects PCCA 2-nr. 166/2012 and ENIAC 03/2013.

" J. Al-zanganawee acknowledges the support from the ministry of the Higher Education and Scientific Research of Iraq."

#### References

- [1] K. Besteman, J. Lee, F. wiertz, H. Heering, C. Dekker, Nano Letters, **3**, 6 (2003).
- [2] K. Balsubramanian, M. Burghard, Anal Bioanal Chem, **385**, (2006).
- [3] S. Jain, S. Singh, D. Horn, V. Davis, M. Ram, S. Pillai, J.Biosens.Bioelectron., **S:11**, (2012).
- [4] C. Nami, U. Takayuki, N. Hidehiro, I. Takao, M. Wataru, A. Seiji, N. Yoshikazu, I. Mitsuru, T. Hiroshi, Jpn.J.Appl.Phys, **39**, (2000).
- [5] D. Dorobantu, P. Bota, M. Badea, I. Boerasu, D. Bojin, M. Enachescu, Proceedings of the 37<sup>th</sup>

- Annual Congress of the American Romanian Academy of Arts and Sciences (ARA)., June, (2013)
- [6] A. Star, J. Gabriel, K. Bradley, G. Gruner, *Nano letters*, **3**, 4 (2003).
  - [7] J. Kong, A. Cassell, H. Dai, *Chemical Physics Letters*, **292**, (1998).
  - [8] C. Liu, Y. Fan, M. Liu, H. Cong, H. Cheng, M. Dresselhaus, *Science*, **286**, 5442 (1999).
  - [9] W. Maser, E. Muñoz, A. Benito, M. Martínez, G. de la Fuente, Y. Maniette, E. Anglaret, J. Sauvajol, *Chemical Physics Letters*, **292**, issue 4-6 (1998).
  - [10] P-M. Bota, D. Dorobantu, I. Boerasu, D. Bojin, M. Enachescu, *Surface Engineering and Applied Electrochemistry.*, **50**, 4 (2014),
  - [11] M. kusaba, Y. Tsunawaki, *Thin solid films.*, **506-507**, (2006).
  - [12] V. Le Borgne, B. Ar`ssa, M. Mohamedi, Y. Kim, Morinobu Endo, M. El Khakani, *J Nanopart Res.*, **13**, (2011).
  - [13] P-M Bota, D. Dorobantu, I. Boerasu, D. Bojin, M. Enachescu, *Materials Research Innovations*, **19**, 1 (2015).
  - [14] S. Costa, E. Borowiak-Palen, M. Kruszynska, A. Bachmatiuk, R. Kalenczuk, *Materials Science-Poland*, **26**, 2 (2008).
  - [15] K.Safarova, A.Dvorak, R. Kubinek, M.Vujtek, A. Rek, *Modern Research and Educational Topics in Microscopy*, **1**, (2007).
  - [16] I. W. Chiang, B. E. Brinson, A. Y. Huang , P. A. Willis, M. J. Bronikowski , J. L. Margrave, R. E. Smalley, R. H. Hauge, *J. Phys. Chem. B*, **105**, 35 (2001).
  - [17] D. Dorobantu, P-M Bota, I. Boerasu, D. Bojin, M. Enachescu, *Surface Engineering and Applied Electrochemistry*, **50**, 5 (2014)